Compliance Analysis of Series Arc-fault in AFCI-Equipped Inverters in Accordance with IEC 63027

Filipe F. Ramos, *Student Member*, *IEEE*, Jose C. S. A. Neto, Fabio J. M. Almeida, Silvia M. S. G. Velázquez, and Bruno L. S. Lima

***Abstract*— The National Institute of Metrology, Quality and Technology (*Instituto Nacional de Metrologia, Qualidade e Tecnologia* - INMETRO) introduces that, starting in 2024, all photovoltaic (PV) inverters sold in the Brazilian market must incorporate an Arc-Fault Circuit Interrupt (AFCI) function into their systems. These inverters are required to comply with the IEC 63027:2023 (Photovoltaic power systems – DC arc detection and interruption) standard. Considering this, the Electrical Engineering Laboratory at Mackenzie Presbyterian University (*Universidade Presbiteriana Mackenzie* – UPM) conducted a series of arc-faults tests on three inverters available in the market, following the IEC 63027 standard. Each of the three inverters underwent a total of 32 arcs, considering number of Maximum Power Point Tracking (MPPT) ports, different impedance topologies, arc position in the PV system, and maximum values of voltage and current. The experiments revealed that two of the three inverters are not capable of meeting the international standard for detecting and interrupting series arc-faults, highlighting the need evaluation of PV inverter sold in the Brazilian market. During the analysis, it was noted that for certain parameters proposed by IEC 63027, there is a gap of information regarding evaluation of the data relating to arc self-extinguish or actual AFCI intervention. It is show that this scenario can raise a concern: the possibility exists for an inverter meet the international standard without implementing an effective AFCI technology. The 96 tests conducted were compared in terms of arc detection time and arc energy. The data were analyzed and compared with respect to the phenomena of arc self-extinguishing and the operation of the AFCI. Suggestions for enhancements to the IEC 63027 standard were provided.**

Link to graphical and video abstracts, and to code: https://latamt.ieeer9.org/index.php/transactions/article/view/8821

***Index Terms*— IEC 63027, AFCI, DC arc-fault detection, series arc-fault, photovoltaics (PVs) systems.**

I. Introduction

In Brazil, the demand for photovoltaic (PV) installations has surged remarkably over the past six years. By 2023, PV generation accounted for 16.1% of the entire Brazilian energy matrix [1].

This work was financed by Huawei Technologies Co. Ltd with Electrical Engineering Laboratory at Mackenzie Presbyterian University, under the Information Technology Law (Law No. 13.969, dated December 26, 2019, Brazil). *(Corresponding author: Filipe F. Ramos).*

F. F. Ramos, J. C. S. A. Neto, F. J. M. Almeida, S. M. S. G. Velázquez, and B. L. S. Lima are with the Mackenzie Presbyterian University, São Paulo, Brazil (e-mails: filipe.ramos@mackenzie.br, jose.almeida@mackenzie.br, fabio.almeida@mackenzie.br, silviamaria.velazquez@mackenzie.br, and bruno.lima@mackenzie.br).

Due to this increase, accidents related to PV systems are also expected to rise [2-6].

A notable risk in these installations is the potential occurrence of arc-faults [5-6], particularly series arcs, due to the characteristic of PV systems having many series connections. An electrical arc is hazardous and can lead to fires if not promptly detected and interrupted [3][4].

Since 2011 in response to arc-faults risks, the National Electrical Code (NEC) in its Section 690.11, mandated that PV installations on buildings with an electrical voltage of 80 volts or higher must include an Arc Fault Circuit Interrupter (AFCI) [7]. Subsequently, photovoltaic equipment, such as string inverters, began to integrate AFCI technology into their systems. These inverters, in turn, underwent testing to verify their arc detection capabilities [8-10].

The UL 1699B:2011 standard outlines the criteria and procedures for testing, aiming to evaluate and ensure the ability of these devices to detect and interrupt arc-faults in PV systems [10]. Subsequently revised in 2018, the UL 1699B has established the reference for series arc fault testing procedures in PV systems in the United States [11].

GB-t 39750 (2021) is a regulation from China that focuses on arcs in photovoltaic systems, both series and parallel. It does not enforce specific protections for parallel arcs but offers a framework for testing and approving safety devices [11][12].

A study at Sandia National Laboratories [8] tested arc fault protection devices in photovoltaic systems according to the UL 1699B. The tests evaluated the efficacy of an AFCI across various PV configurations, focusing on detection capability and resistance to nuisance tripping.

In [13], Sandia National Laboratories and Tigo Energy investigates unwanted tripping in UL 1699B-listed arc-fault detection devices (AFDs) in PV systems through laboratory tests. Results revealed that many devices are prone to unwanted tripping or fail to detect hazardous arc-fault events.

Published in May 2023 by the International Electrotechnical Commission (IEC), the IEC 63027 (Photovoltaic power systems – DC arc detection and interruption) introduces new testing parameters for equipment used in the detection and interruption of arc-faults in PV systems [14]. Moreover, this standard addresses issues such as varying impedance topologies in PV systems, the positioning of the electrical arc in the system, and the maximum reaction time for system interruption.

In [11], a comprehensive analysis of the IEC 63027, UL 1699B, and GB-t 39750 standards is provided, detailing

their comparative advantages and disadvantages. The IEC 63027 offers a globally recognized framework focusing on series arcs in photovoltaic systems, with stringent testing requirements and broad protection guidelines. The UL 1699B standard emphasizes series arc protection and mandates testing on both positive and negative poles, enhancing safety in the US context. Meanwhile, the Chinese GB-t 39750 standard covers both series and parallel arcs. These standards differ significantly in fault location testing, reconnection methods, and the specificity of protection requirements, reflecting varied regulatory priorities and practices across regions.

A. Motivation and Problem Statement

In the Brazilian context, while the standard ABNT NBR16690:2019 (Electrical Installations of Photovoltaic Arrays - Design Requirements) highlights the dangers of arc-faults, it does not yet mandate the use of AFCI-equipped devices [15]. Given this context, and with over 35,739 MW of photovoltaic energy already installed in Brazil [1], the market faces an imminent problem, and measures must be taken to enhance safety in these installations.

Accordingly, in November 2023, the National Institute of Metrology, Quality and Technology (*Instituto Nacional de Metrologia, Qualidade e Tecnologia* - INMETRO) issued Ordinance No. 515, introducing new requirements for protection against series arc-faults [16]. Starting in 2024, PV inverters sold in the Brazilian market must comply with the IEC 63027 standard concerning the detection and interruption of series arc-faults in PV systems [16].

As the application of the IEC 63027 procedure is a novelty for equipment testing internationally, the worldwide community would benefit from information regarding the application of the standard procedures.

B. Contribution

As equipment testing according to the IEC 63027 procedure was developed at the Electrical Engineering Laboratory at UPM on three string inverters available in the Brazilian market, presenting their performance in the event of a series electrical arc. It was found that 2 of the 3 inverters did not meet the international standard for detecting electric arcs in series, however the inverters which did not pass the criteria presented ambiguous results for low current arc tests, which had no instructions on better evaluation regarding the procedures on IEC 63027 standard.

During tests with a low current, it was found that there is a possibility of the arc extinguishing itself and masking the intervention of the inverters' AFCI function. Improvements to IEC 63027 were suggested to mitigate this situation, such as better evaluation of the results regarding current curve behavior, examples of self-extinguish arc are presented, as well as increasing the curve base current and

The remainder of this article is structured as follows. Section II introduces the fundamentals of arc-faults in PV systems and reviews significant research in arc-fault detection. Section III outlines the methodology employed in this study, detailing the test bench, testing parameters, and key aspects of the IEC 63027 standard. Section IV presents the experimental results, along with their analysis and implications. Finally, Section V concludes the article.

II. Arc-Faults in PV Systems

An electric arc can be described as "A discharge of electricity through a gas, normally characterized by a voltage drop in the immediate vicinity of the cathode approximately equal to the ionization potential of the gas" [17][18]. An arc-fault can reach temperatures of several thousand degrees Celsius [18].

Alternating current (AC) arc-faults exhibit self-extinguishing properties due to voltage and current passing through zero potential. In contrast, direct current (DC) arc-faults in photovoltaic (PV) systems tend to burn steadily, posing a fire risk. Also, theses arcs-faults can produce electrical noise, which can be detectable in conductors.

The occurrence of arc-faults in PV systems can result from various causes. Poorly executed connections, improperly crimped or tightened cables, or the use of components from different manufacturers can create failure points, making the system susceptible to arc formation [3-5]. Additionally, damage by rodents can compromise cables, introducing potential vulnerabilities.

The NBR 16690 standard identifies three types of arc-faults that can occur in a PV installation: series arcs, parallel arcs, and ground arcs. Fig. 1 illustrates these failures in a PV circuit [15].

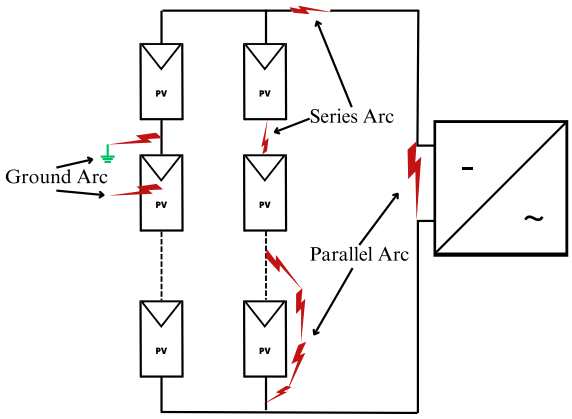

Fig. 1. Types of electrical arcs in a PV system, adapted from [15].

Series arcs, often resulting from poor connections or compromised cabling, are likely in PV systems due to the high number of series connections present [15]. If not rapidly extinguished, a series arc can generate a parallel arc, as the series arc may spread to adjacent conductors.

Parallel arcs typically stem from a short circuit between the positive and negative cables in the DC part of the circuit, often originating from cable insulation degradation. This type of arc-fault is more complex than series arcs [19], yet less common due to standards requiring double-insulated cables in PV installations [15].

Ground arcs result from insulation failure causing

positive and negative connections to contact the earth potential. Like parallel arcs, ground arcs are relatively rare occurrences.

A. State of the Art

The UL1699B and IEC 63027 standards do not prescribe or limit a specific method for detecting an arc-fault.

All PV systems are influenced by various conditions that affect current and voltage signals, including light intensity changes, inverter switching, types of connectors and modules, cabling length, and the number of PV modules. These factors complicate the development of arc detectors. Recent solutions rely on the application of artificial intelligence (AI), machine learning (ML), and deep learning (DL) algorithms to analyze patterns and identify arc signals across different system topologies.

A comprehensive review by [20] examines several failures and detection methods in PV systems. This study highlights the use of wavelet transforms (WT) and machine learning (ML) for detecting series arc-faults. [21] presents a current demodulation algorithm for improving arc fault detection in photovoltaic (PV) systems, the method isolates arc fault noise by filtering out the inverter's switching signal. [22] employed the Chirp Z-Transform (CZT) to investigate and characterize the feasibility of low-frequency spectral analysis of the current in PV systems. [23] proposes the use of WT and conducts an experimental comparison of WT with the Fast Fourier Transform (FFT). [24] presents a methodology for DC series arc fault diagnosis in photovoltaic systems using domain adaptation combined with deep convolutional generative adversarial networks (DA-DCGAN). [24] constructs a data-driven model trained on normal and arcing data from a source domain and normal data from a target domain. [25] investigates the detection of series DC arc faults using a hybrid method combining time-domain and discrete wavelet transform (DWT) analyses. In [26] the performances of eight machine learning algorithms were compared, and five time-domain features were extracted to detect arc faults in DC systems, highlighting the effectiveness of different methods under various operating conditions and load types. [27] discusses the use of DL techniques to diagnose arc faults in DC distribution systems and predict circuit behavior in real-time. [27] transformes measured time series into time-frequency domain sequences using STFT, then this sequences are input into a Convolutional neural network (CNN) model and an long short-term memory network (LSTM) model. [28] proposes a time-domain technique based on mathematical morphology called the decomposed open–close alternating sequence (DOCAS). [29] presents a method for series DC arc fault detection using ensemble machine learning (EML) algorithms. Time-domain features, such as average, median, variance, RMS, and max-min difference, are extracted from the experimental data.

B. DC Arc Model

The model developed by Stokes and Oppenlander is a well-known study of free-burning arcs between series electrodes in open air [30][31]. Stokes and Oppenlander formulated the arc behavior in Equation 1, which relates the DC arc fault current and voltage.

$$V_{arc} = (20 + 0{,}534 z_g) I_{arc}^{0.12} \quad (1)$$

The equation's 1 parameters are defined as follows:
V_{arc} is the arc voltage;
I_{arc} is the arc current and;
z_g is the length of the arc gap (in mm).

[31] reviews various DC arc models and their applications in estimating incident energy for arcing faults. It compares the formulations of DC-arc resistance across different models, including those for free-burning arcs in open air and those within enclosed environments.

III. Methodology

This study involves a series of tests conducted in accordance with the IEC 63027 standard on three string inverters (Inverter A, B, and C) available in the Brazilian market. The experiments were carried out at the UPM electrical engineering laboratory in São Paulo, SP.

A. Tests Setup

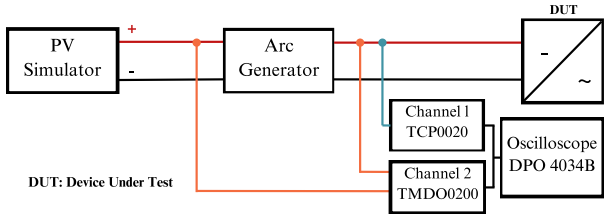

Fig.2. Schematic diagram of the monitoring system.

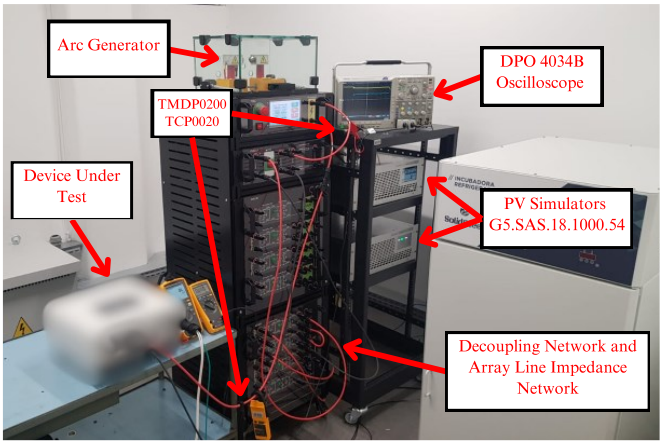

Fig. 3. Scheme of the laboratory test bench.

For conducting the tests in a controlled laboratory environment, two Regatron G5.SAS.18.1000.54 PV simulators were used to simulate PV arrays. Additionally, an arc-faults generation system comprising three modules was employed: a decoupling network, a line impedance network, and the arc generation system itself with a ball-ring electrode pair made of tungsten alloy, as required by IEC 63027.

Monitoring of the tests involved a Tektronix DPO 4034B oscilloscope. The arc current was monitored using a TCP0020 probe, and the voltage across the electrodes was

measured with a TMDP0200 probe. Measurements were taken over a 4-second window, capturing 100,000 points at a 25k sample rate. The monitoring system's diagram is illustrated in Fig. 2 and Fig. 3 displays the setup used for these tests.

B. Test Procedures and Parameters

The methodology of this study adheres to Section 9.2.6 "Test procedure" of the IEC 63027 standard. Table I specifies the necessary parameters for conducting the tests, including current, voltage, electrode spacing, and electrode separation rate.

Based on the maximum current and voltage operation specifications of the inverters, the tests from Table I were applied to the Device Under Test (DUT). For this research, the three chosen inverter models have voltage, current, and number of Maximum Power Point Tracking (MPPT) inputs as outlined in Table II.

The IEC 63027 identifies four different models of PV generators: Half string model, Full string model, Module-based model, and Parallel string model. In this study, the selected inverters correspond to the Half string generation model. Fig. 4 illustrates the configuration used to test each MPPT input of the inverter. Table III details the values of each component shown in Fig. 4.

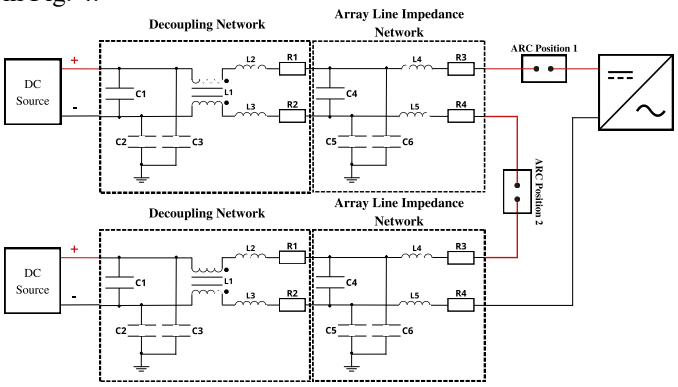

Fig. 4. Single string test setup, arc positioned before inverter (ARC position 1) and positioned in the middle of the strings (ARC position 2).

As show in Table III, two potential values for component C4 are provided, as per IEC 63027. The different values of this component represent various frame and module technologies. Depending on the DUT's arc detection method, a higher or lower capacitance in the circuit may present a positive or negative impact for arc detection.

According to data from Tables I and II, it was identified that the three selected inverters meet the criteria only for tests 1 and 2 showed in Table I. Consequently, each MPPT input of the inverters underwent the following sequence of tests: two tests involved placing the arc-fault directly in series with the positive MPPT input of the inverter using a 300nF C4 component, and two additional tests using a 20nF C4 component. Similarly, another set of tests positioned the arc-fault in the middle of the PV string, also using 300nF and 20nF C4 components for two tests each, as illustrated in Fig. 4. This total of 8 tests for each test type in Table I, with each test sequence conducted for each MPPT input of the inverter.

For the arc fault evaluation limits in Section 8.1.3 “Operation in case of series arc fault event” of IEC 63027, a maximum arc detection time of 2.5 seconds or before the arc reaches 750 J is required. Therefore, a minimum electrode spacing time of 2.7 seconds was established to ensure the inverter has sufficient time as defined by the standard to detect and extinguish the arc-fault. After 2.7 seconds, the electrodes separate to 50 mm, marking the end of the test.

TABLE I
ARCING TEST CONDITIONS, ADAPTED FROM [14]

Test #	I_{arc} (A)	I_{mpp} (A)	Sep. Rate (mm/s)	V_{mpp} (V)	V_{oc} (V)	$R_{tot}(\Omega)$	Gap (mm)
1	2.5	3.0	2.5	312.0	480.0	56.0	0.8
2	7.0	8.0	5.0	318.0	490.0	21.0	0.8

TABLE II
PLATE DATA FOR THE INVERTERS TESTED

Inverter	A	C	B
Power	5000 W	5000W	5000 W
Maximum DC voltage V_{oc}	600 V	550V	550 V
MPPT voltage range V_{mpp}	90 ~ 560 V	60 ~ 550 V	70 ~ 550 V
Maximum input current	12,5 A	13,5 A	13,0 A
Number of MPPT	2	2	2

TABLE III
COMPONENT PARAMETERS, ADAPTED FROM [1]

DC source decoupling network and Array line impedance network			
Component	Value	Component	Half String
$C1$	20 µF	$C4$	300 nF *or* 20 µF
$C2, C3$	22 nF	$C5, C6$	0,5 nF
$L1$	12 mH	$L4, L5$	25 µH
$L2, L3$	60 µH	$R4, R4$	$Max.$ 0,5 Ω
$R1, R2$	0 Ω		

As per IEC 63027, Section 9.2.7 “Arc energy and response time measurement,” the electric arc between electrodes is considered to commence when the electrode voltage reaches 10 V and ends when the arc current drops below 250 mA. To detect the arc's occurrence, a trigger on oscilloscope channel 2 was set at 10V with a horizontal position of 0.802 seconds.

C. Arc Energy Calculation and Data Analysis

An algorithm was developed in MATLAB for the analysis of the data gathered, which collects voltage, current, and time measurements from the oscilloscope for analysis. The calculation of the arc energy utilized Equation

2.

$$E = \sum_{i=1}^{n} V_i . I_i . (t_i - t_{i-1}) \quad (2)$$

The equation's 2 parameters are defined as follows: E: energy of the arc, expressed in joules (J); v: arc voltage, expressed in volts (V); I: arc current expressed in amperes (A); t: instant of time, expressed in seconds (s); n: number of samples from the start to the end of the arc-fault event.

The developed system analyzes the period from the initiation of the arc to the moment it extinguishes. It is crucial to note that the arc may persist even during the final electrode separation, potentially resulting in an arc duration exceeding 2.7 seconds.

IV. Tests, Results and Discussions

Inverters A and C feature AFCI functionality as stated in their manuals and offer the option to enable this feature in their configuration menus. Inverter B, however, lacks any mention of AFCI in its documentation. For Inverters A and C, the AFCI protection options were activated, while Inverter B was tested with its default factory settings.

The three inverters chosen for this study are specified only for Test type 1 and Test type 2. The results of these tests are presented in Table IV. Consequently, a total of 32 tests were conducted for each inverter.

Fig. 5. Arcs generated during tests. Test type 1 is shown on the left and Test type 2 on the right.

A. Inverter A

None of the tests conducted on Inverter A exceeded the 2.5-second maximum duration. Furthermore, none of the tests surpassed the maximum power threshold of 750 joules.

For test type 1, tests number 1, 6, and 15 had an average extinction time of 0.143 seconds, with arc behavior as presented in Fig. 6, while the average extinction time for the other tests in Test type 1 was 0.038 seconds, with arc behavior as presented in Fig. 6. Comparing the arc behavior in Fig. 6 is possible to verify that the arcs in tests 1, 6, and 15 were extinguished by the AFCI, presenting a characteristic current decay, whereas the others in Test type 1 were extinguished naturally presenting a sudden current peak followed by a cease of the arc current.

For test type 2, the average arc extinction time was 0.164 seconds. Also, according to the current curve for Tests type 2, it is possible to verify the same current decay from the AFCI intervention, as seem from the curves in Tests type 1.

B. Inverter B

The tests conducted on Inverter B are detailed in Table IV. During tests 1 to 16, the average duration of the arc-fault was 1.495 seconds. In tests 1, 3, 4, 5, 6, 7, and 11, the arc duration exceeded the 2.5-second. However, none of these tests surpassed the maximum energy limit of 750 joules.

In tests 17 to 32, the average arc duration was 3.198 seconds, the maximum observation time for the arc, exceeding the 2.5-second limit in all cases and exhibiting an arc behavior as presented in Fig. 7. The average energy for these tests was 536 joules, within the prescribed standard limit.

Difficulty in sustaining the arc was observed in tests 10, 12, and 14, with an average arc extinction time of 0.046 seconds, with behavior similar to those from the tests on inverter A, with arcs being extinguished naturally. Tests 2, 8, 9, 13, 15, and 16 had an average extinction time of 0.385 seconds, indicating the formation of more well-defined arcs, but also presenting a self-extinguish behavior. For Test type 2, all the tests presented a sustained arc as presented in Fig. 7.

C. Inverter C

In tests 1 to 16, the average duration of the arc-fault was 0.223 seconds, with none of the tests exceeding the maximum arc duration of 2.5 seconds or the maximum energy limit of 750 joules.

In tests 17 to 32, the average arc duration again was 3.198 seconds, exceeding the 2.5-second threshold in every test. The average energy level in this group was 614 joules, staying within the normative upper limit.

In the scope of test type 1, difficulty in sustaining the arc was observed in tests 1, 6, 8, 11, 14, 15 and 16, with an average arc extinction time of 0.043 seconds, similar to those measured in the tests of inverter A and B. However, all arcs in the scope of Test type 1, extinguished naturally, with arc behavior as presented in Fig. 8. For Test type 2, all the tests presented a sustained arc as presented in Fig. 8, with behavior similar to those in Fig 7.

D. Analysis of Results

The results demonstrate that only inverter A was able to extinguish the arc-faults, in both test type 1 and test type 2, within the limits established by IEC 63027. However, it was noted that tests within the scope of test type 1, 77% of the conducted tests presented an arc self-extinguish behavior with the gap specification for this test type. To evaluate whenever the arc was self-extinguished or the inverter AFCI actuated, the arc behavior from tests type 1 configuration were compared as seem in Fig 6. Analyzing Fig. 6, the data from curves in (a) demonstrate a current spike followed by an abrupt cease of the arc current, as for curves in (b) there is a gradual current decay resulted from the AFCI intervention.

While self-extinguishing indicates compliance, it raises a critical concern: the possibility exists for inverter meet the standard without implementing an effective AFCI technology.

As an example, if an inverter has four inputs instead of two, it could potentially only be subject to test type 1 (as per

Table I) and show compliance with the standard without the need to be subject to type 2 tests. For instance, Inverter C, which failed to meet the criteria in test type 2, may pass the requirements with such a modification, benefitting from the arc self-extinguishing behavior for test type 1 parameters. Fig. 9 illustrate the proposed argument.

In this context, inverter manufacturers may have two viable options. The first is to reduce the input current, as illustrated in Fig. 9. Alternatively, they could implement a more advanced and robust AFCI function. This latter approach would not only

TABLE IV
TEST RESULTS

Parameters					Inverter A		Inverter B		Inverter C	
Test #	Test Type	MPPT Input	Arc Position	C4 Value	Arc Duration Time [s]	Arc Energy [J]	Arc Duration Time [s]	Arc Energy [J]	Arc Duration Time [s]	Arc Energy [J]
1	1	1	S	330 nF	0.141	5.982	3.011	199.321	0.073	3.586
2	1	1	S	330 nF	0.085	4.086	0.667	36.651	0.214	13.138
3	1	1	S	20 uF	0.050	1.256	2.688	155.981	0.845	53.263
4	1	1	S	20 uF	0.040	0.600	3.105	215.202	0.346	21.015
5	1	1	M	330 nF	0.051	0.284	3.198	195.125	0.335	21.429
6	1	1	M	330 nF	0.145	8.314	3.198	210.058	0.045	1.346
7	1	1	M	20 uF	0.063	2.165	3.198	175.011	0.444	31.319
8	1	1	M	20 uF	0.002	0.036	0.297	15.833	0.040	1.312
9	1	2	S	330 nF	0.033	1.053	0.262	14.614	0.185	9.295
10	1	2	S	330 nF	0.027	0.838	0.038	0.533	0.168	8.439
11	1	2	S	20 uF	0.019	0.122	3.071	210.511	0.032	0.444
12	1	2	S	20 uF	0.013	0.093	0.031	0.322	0.631	47.372
13	1	2	M	330 nF	0.018	0.236	0.319	21.498	0.106	4.921
14	1	2	M	330 nF	0.021	0.870	0.069	2.026	0.060	1.806
15	1	2	M	20 uF	0.143	6.308	0.434	27.535	0.033	0.906
16	1	2	M	20 uF	0.070	3.673	0.333	20.037	0.019	0.134
17	2	1	S	330 nF	0.154	17.180	3.198	456.253	3.198	602.985
18	2	1	S	330 nF	0.141	16.615	3.198	499.018	3.198	558.692
19	2	1	S	20 uF	0.109	10.759	3.198	506.484	3.198	526.397
20	2	1	S	20 uF	0.110	11.868	3.198	493.437	3.198	587.328
21	2	1	M	330 nF	0.284	37.728	3.198	524.046	3.198	582.579
22	2	1	M	330 nF	0.271	35.192	3.198	498.782	3.198	685.289
23	2	1	M	20 uF	0.151	19.485	3.198	436.442	3.198	661.430
24	2	1	M	20 uF	0.124	15.926	3.198	500.466	3.198	666.148
25	2	2	S	330 nF	0.179	24.250	3.198	533.394	3.198	535.207
26	2	2	S	330 nF	0.136	14.838	3.198	450.855	3.198	579.300
27	2	2	S	20 uF	0.109	12.217	3.198	600.167	3.198	545.091
28	2	2	S	20 uF	0.124	13.142	3.198	494.997	3.198	653.309
29	2	2	M	330 nF	0.273	38.777	3.198	650.204	3.198	653.309
30	2	2	M	330 nF	0.229	30.514	3.198	613.636	3.198	688.453
31	2	2	M	20 uF	0.128	13.274	3.198	658.944	3.198	651.563
32	2	2	M	20 uF	0.106	12.014	3.198	664.751	3.198	653.818

Note: In the "Arc Position" column, "S" refers to the position of the arc at the inverter input, as shown in Fig. 4, while "M" refers to the arc between the strings, as shown in Fig. 4.

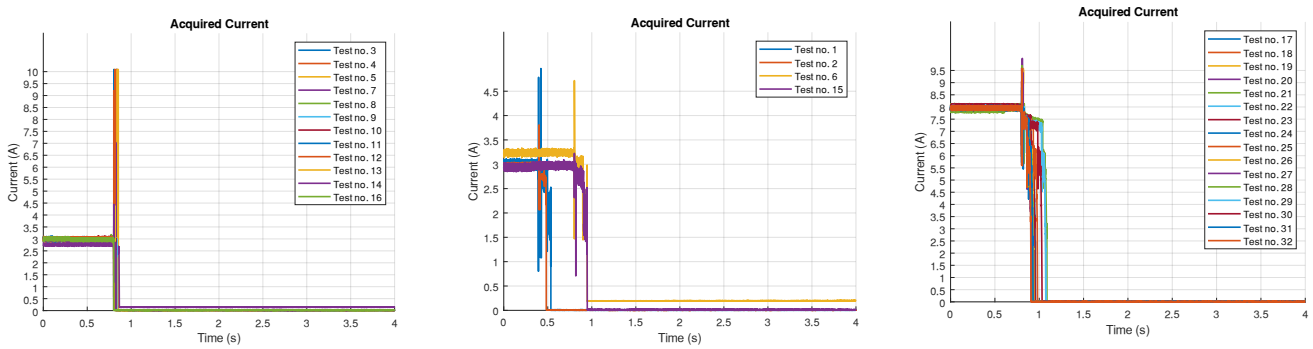

(a) (b) (c)

Fig. 6. Arcs generated during tests in inverter A. (a) arcs were extinguished with immediate electrode separation (b) arcs were extinguished by AFCI for Test type 1 configuration (c) arcs were extinguished by AFCI for Test type 2 configuration.

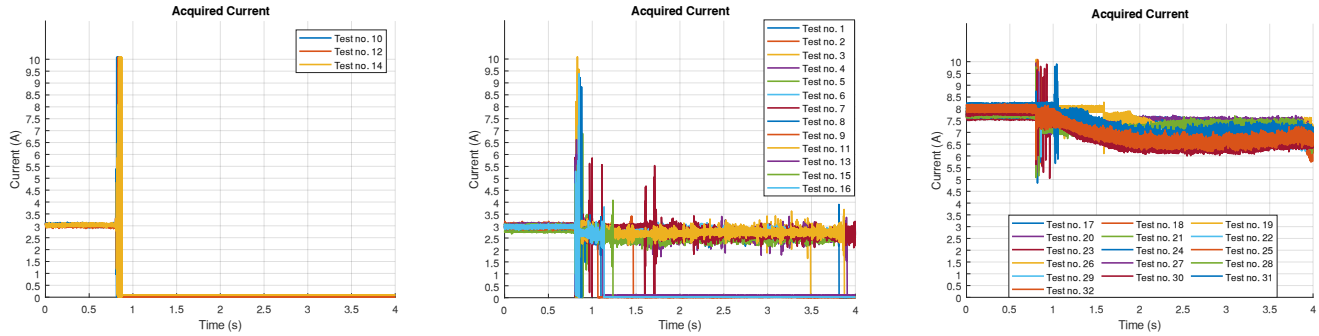

(a) (b) (c)

Fig. 7. Arcs generated during tests in inverter B. (a) arcs were extinguished with immediate electrode separation (b) arcs were not extinguished by AFCI for Test type 1 configuration (c) arcs were not extinguished by AFCI for Test type 2 configuration.

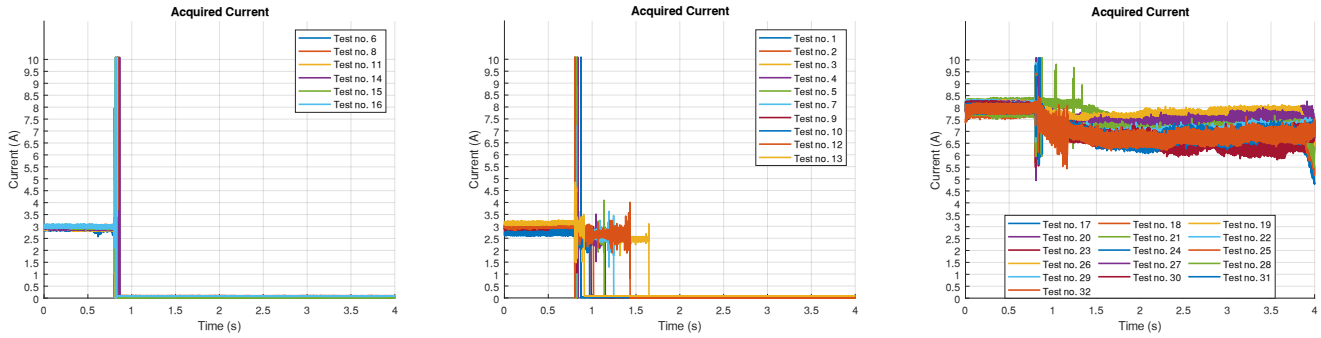

(a) **(b)** **(c)**

Fig. 8. Arcs generated during tests in inverter C. (a) arcs were extinguished with immediate electrode separation (b) arcs were extinguished naturally for Test type 1 configuration (c) arcs were not extinguished by AFCI for Test type 2 configuration.

comply with current standards but also significantly enhance the safety and reliability of the inverters, addressing the critical need for effective prevention of electrical fires caused by arc faults.

E. Suggestions for Improvement to the IEC 63027

To mitigate the uncertainty regarding detection present in the tests under Test 1 and to construct a more robust standard, the authors suggest the following topics for consideration by the technical committees:

For the tests under test type 1 parameters a reduction in the gap between the electrodes and/or a reduction in the separation rate can create a better condition for low power arc self-sustenance, as the gap has direct impact on the arc voltage and current as indicated by Equation (1). An increase in current can also solve the problem of natural extinguishing.

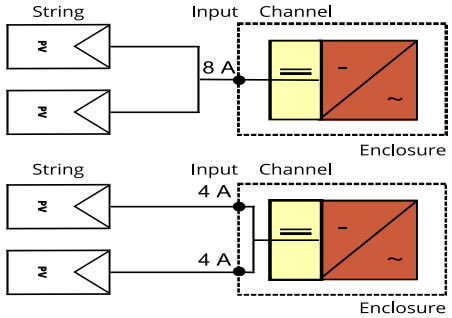

Fig. 9. Possible measure to make the inverter not subject to the type 2 tests.

A statistical study of arc formation under reduced gap, separation rate and with increased current, can lead to more appropriate parameter values for test type 1 evaluation.

Also, evaluation criteria based on the current behavior during tests is useful for reporting the AFCI intervention, as the self-extinguishing arc current has a characteristic behavior as presented in Fig. 6 (a), Fig. 7 (a) and Fig. 8 (a), and this type of behavior can be discarded with the curve analysis.

V. Conclusion

This study has experimentally revealed limitations in the arc-fault protection resources in inverters commercialized in Brazil. The AFCI technological gap in inverters available in the Brazilian market raises concerns about the future safety of PV installations in the country.

The study demonstrated that 2 out of 3 inverters failed to meet the requirements set by the relatively new IEC 63027 standard. In terms of the IEC 63027 tests, it was presented that, while possible, there is difficulty in distinguishing between the natural extinguishing of the arc-faults and the activation of the AFCI of the inverter in the context of test type 1 parameters.

Due to the parameters of test type 1 (separation rate, spacing, current, and voltage), it was noted that the arc-faults could extinguish without the intervention of the AFCI function. This issue might be attributed to the parameters proposed by the standard itself or the type of switching used by the inverter in the DC to AC conversion. In test type 2, it became clear whether the inverter possesses a function to suppress the arc, as was observable in the analysis of Inverter A compared to the others.

Regarding the IEC 63027 standard, a better evaluation of the parameters for test type 1, such as the gap between electrodes, should be reviewed, also considerations regarding the current behavior during tests could benefit the evaluation process of PV inverters.

Also, the study presented demonstrates that the PV inverters commercialized in Brazilian market still do not possess AFCI technology, despite the earliest standard for this subject being published in 2011. This means that most of the inverters commercialized in Brazil should be subject to firmware and hardware modifications to meet AFCI criteria. However, according to current the standards, the modifications can be made to benefit from arc self-extinguish instead of implementing AFCI.

Acknowledgments

The Electrical Engineering Laboratory at Mackenzie Presbyterian University is partially funded by research and development projects. This work was financed under the Information Technology Law (Law No. 13.969, dated December 26, 2019, Brazil) in the Inova Solar: Mackenzie – Huawei project in partnership with Huawei Technologies Co. Ltd, to whom the authors extend their humble gratitude.

Data

The data from this study will be made available upon request.

References

[1] ABSOLAR - Brazilian Photovoltaic Solar Energy Association. (2024, jul. 23). *Panorama of solar photovoltaics in Brazil and worldwide*. [Online]. Available: https://www.absolar.org.br/mercado/infografico/

[2] G. Manzini, P. Gramazio, S. Guastella, C. Liciotti, and G. L. Baffoni, "The Fire Risk in Photovoltaic Installations - Test Protocols For Fire Behavior of PV Modules," *Energy Procedia*, vol. 82, pp. 752-758, Dec, 2015. doi: 10.1016/j.egypro.2015.11.805.

[3] Sepanski A. *et al*., "Assessing fire risks in photovoltaic systems and developing safety concepts for risk minimization" 2018. [Online]. Available: https://www.energy.gov/eere/solar/articles/assessing-fire-risks-photovoltaic-systems-and-developing-safety-concepts-risk

[4] R. Backstrom and D. Dini, "Firefighter Safety and Photovoltaic Installations Research Project," Research Project: Firefighter Safety and Photovoltaic Systems, Nov. 2011, doi:10.54206/102376/VIYV4379.

[5] Z. Wu, Y. Hu, J. X. Wen, F. Zhou and X. Ye, "A Review for Solar Panel Fire Accident Prevention in Large-Scale PV Applications", *IEEE Access*, vol. 8, pp. 132466-132480, 2020, doi: 10.1109/ACCESS.2020.3010212

[6] S. S. Nair, "A Survey report of the firefighters on fire hazards of PV fire," 2018 IEEE International Conference on System, Computation, Automation and Networking (ICSCA), Pondicherry, India, 2018, pp. 1-5, doi:10.1109/ICSCAN.2018.8541219.

[7] *National Electrical Code*, NFPA70, National Fire Protection Association, Batterymarch, MA, 2011.

[8] J. Johnson et al., "Photovoltaic DC Arc Fault Detector testing at Sandia National Laboratories," 2011 37th IEEE Photovoltaic Specialists Conference, Seattle, WA, USA, 2011, pp. 003614-003619, doi: 10.1109/PVSC.2011.6185930.

[9] K. J. Lippert and T. Domitrovich, "AFCIs - From a standards perspective," 2013 IEEE IAS Electrical Safety Workshop, Dallas, TX, USA, 2013, pp. 57-61, doi: 10.1109/ESW.2013.6509004.

[10] Underwriters Laboratories Inc., Subject 1699B, Outline of Investigation for Photovoltaic (PV) DC Arc-Fault Circuit Protection, Issue Number 1, 2011.

[11] J. L. Putzke, L. Michels and L. V. Bellinaso, "Electric Arcs in Photovoltaic Systems: A Comparative Analysis of IEC 63027, UL 1699B, and GB-t 39750 Standards," *2023 IEEE 8th Southern Power Electronics Conference and 17th Brazilian Power Electronics Conference (SPEC/COBEP)*, Florianopolis, Brazil, 2023, pp. 1-5, doi: 10.1109/SPEC56436.2023.10407946.

[12] *GB/T 39750-2021 - Technology requirements of DC arc-fault circuit protection for photovoltaic power system*, National Standard of the People's Republic of China Std., 2021.

[13] J. Johnson, K. M. Armijo, M. Avrutsky, D. Eizips and S. Kondrashov, "Arc-fault unwanted tripping survey with UL 1699B-listed products," 2015 IEEE 42nd Photovoltaic Specialist Conference (PVSC), New Orleans, LA, USA, 2015, pp. 1-6, doi: 10.1109/PVSC.2015.7356427.

[14] *IEC 63027 ed. 1b: Photovoltaic Power Systems - DC Arc Detection and Interruption*, International Electrotechnical Commission Std., 2023.

[15] *ABNT NBR 16690 ed. 1 - Electrical installations of photovoltaic systems - Project requirements*, Brazilian Association of Technical Standards Std., 2019.

[16] National Institute of Metrology, Quality and Technology. (2023, Nov. 10). *INMETRO Ordinance number 515*. [Online]. Available: http://www.inmetro.gov.br/LEGISLACAO/detalhe.asp?seq_classe=1&seq_ato=3010.

[17] IEEE Standard Definitions of Terms Relating to Corona and Field Effects of Overhead Power Lines, IEEE Std. 539-2020, 2021, doi: 10.1109/IEEESTD.2021.9513501.

[18] K. T. Compton, "The Electric Arc", *Transactions of the American Institute of Electrical Engineers*, vol. XLVI, pp. 868-883, Jan.-Dec. 1927, doi: 10.1109/T-AIEE.1927.5061428.

[19] J. Flicker and J. Johnson, "Electrical simulations of series and parallel PV arc-faults," 2013 IEEE 39th Photovoltaic Specialists Conference (PVSC), Tampa, FL, USA, 2013, pp. 3165-3172, doi: 10.1109/PVSC.2013.6745127.

[20] Hong, Ying-Yi; Pula, Rolando A.. Methods of photovoltaic fault detection and classification: a review. *Energy Reports*, v. 8, p. 5898-5929, Nov. 2022, doi: 10.1016/j.egyr.2022.04.043.

[21] J. C. Kim, R. Ball and B. Lehman, "Isolation and Detection of Arc Fault Noise in a Real PV System Using Current Demodulation and Autocorrelation Coefficients", *IEEE Transactions on Power Electronics*, vol. 39, no. 8, pp. 10351-10367, Aug. 2024, doi: 10.1109/TPEL.2024.3391420.

[22] Artale G. *et al*., "Characterization of DC series arc faults in PV systems based on current low frequency spectral analysis," *Measurement*, vol. 182, p. 109770, Set. 2021, doi: 10.1016/j.measurement.2021.109770.

[23] Z. Wang and R. S. Balog, "Arc Fault and Flash Signal Analysis in DC Distribution Systems Using Wavelet Transformation", *IEEE Transactions on Smart Grid*, vol. 6, no. 4, pp. 1955-1963, July 2015, doi: 10.1109/TSG.2015.2407868.

[24] S. Lu, T. Sirojan, B. T. Phung, D. Zhang and E. Ambikairajah, "DA-DCGAN: An Effective Methodology for DC Series Arc Fault Diagnosis in Photovoltaic Systems", *IEEE Access*, vol. 7, pp. 45831-45840, 2019, doi: 10.1109/ACCESS.2019.2909267.

[25] X. Yao, L. Herrera, S. Ji, K. Zou and J. Wang, "Characteristic Study and Time-Domain Discrete- Wavelet-Transform Based Hybrid Detection of Series DC Arc Faults", *IEEE Transactions on Power Electronics*, vol. 29, no. 6, pp. 3103-3115, June 2014, doi: 10.1109/TPEL.2013.2273292.

[26] H. -L. Dang, J. Kim, S. Kwak and S. Choi, "Series DC Arc Fault Detection Using Machine Learning Algorithms", *IEEE Access*, vol. 9, pp. 133346-133364, 2021, doi: 10.1109/ACCESS.2021.3115512.

[27] L. Xing, Y. Wen, S. Xiao, D. Zhang and J. Zhang, "A Deep Learning Approach for Series DC Arc Fault Diagnosing and Real-Time Circuit Behavior Predicting,". *IEEE Transactions on Electromagnetic Compatibility*, vol. 64, no. 2, pp. 569-579, April 2022, doi: 10.1109/TEMC.2021.3131670.

[28] M. Kavi, Y. Mishra and M. Vilathgamuwa, "DC Arc Fault Detection For Grid-Connected Large-Scale Photovoltaic Systems", *IEEE Journal of Photovoltaics*, vol. 10, no. 5, pp. 1489-1502, Sept. 2020, doi: 10.1109/JPHOTOV.2020.2998868.

[29] V. Le, X. Yao, C. Miller and B. -H. Tsao, "Series DC Arc Fault Detection Based on Ensemble Machine Learning", *IEEE Transactions on Power Electronics*, vol. 35, no. 8, pp. 7826-7839, Aug. 2020, doi: 10.1109/TPEL.2020.2969561.

[30] R. F. Ammerman, T. Gammon, P. K. Sen and J. P. Nelson, "DC-Arc Models and Incident-Energy Calculations", *IEEE Transactions on Industry Applications*, vol. 46, no. 5, pp. 1810-1819, Sept.-Oct. 2010, doi: 10.1109/TIA.2010.2057497.

[31] A. D. Stokes and W. T. Oppenlander, "Electric arcs in open air," J. Phys. D, Appl. Phys., vol. 24, no. 1, pp. 26–35, Jan. 1991, doi: 10.1088/0022-3727/24/1/006

Filipe Figueiredo Ramos holds a diploma in Electrical Technician from the National Service for Industrial Training (SENAI) (2019). Currently pursuing a degree in Electrical Engineering at the Mackenzie Presbyterian University. Works as a researcher on R&D projects focusing on simulation and characterization of optical modulators. Also involved in research related to the characterization, analysis and safety against arc fault in PV systems. Contributor in technical committees for the development of ABNT (Brazilian Association of Technical Standards) standards.

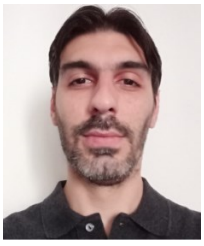

José César de Souza Almeida Neto holds bachelor's degree in electrical engineering with a focus on Energy and Automation from the University of São Paulo (2012), a Master of Sciences and a Doctorate degree in Energy Technology at the Institute of Energy and Environment of the University of São Paulo (2017 and 2023). Has experience in the field of electrical engineering, compliance testing of equipment for photovoltaic application, planning, and project management.

Fábio Jesus Moreira de Almeida holds a Doctorate in Materials Engineering and Nanotechnology (2021), and a master's degree in Nuclear Science and Technology (2006) from the University of São Paulo (USP). Completed undergraduate studies in Physics (2002) and Mathematics (Teaching Degree) (2002) at the UPM (Mackenzie Presbyterian University). Currently serves as a full-time University Professor at the UPM, specializing in areas including Materials, Electromagnetism, Glass, Physics, Mathematics, Calculus, Structures, Mechanics, and Statistics.

Sílvia Maria Stortini González Velázquez, graduated in Chemical Engineering from the Armando Álvares Penteado Foundation (1985), holds a master's degree (2000) and a Ph.D. (2006) in Energy from the Interunit Graduate Program in Energy (PIPGE) of the University of São Paulo

(USP). Adjunct Professor at the School of Engineering of the Mackenzie Presbyterian University. Also involved in research in the field of energy generation from renewable sources: wind, solar thermal and photovoltaic, biomass, biogas, and liquid biofuels.

Bruno Luis Soares de Lima obtained a doctor's and master's degree in electrical engineering from the Polytechnic School of the University of São Paulo (USP) (2017, 2006). Possesses experience in the field of Electrical Engineering, with a focus on electronics, sensors, and electrical automation systems. Currently works as a researcher in R&D projects involving the development of automation systems, sensor networks, and monitoring systems. Also serves as professor of computing and electrical engineering.